Available online at www.sciencedirect.com
SCIENCE DIRECT®
Tetrahedron: Asymmetry
Tetrahedron: *Asymmetry* 16 (2005) 1463–1472

Asymmetric heterogeneous carbene transfer catalyzed by optically active ruthenium spirobifluorenylporphyrin polymers

Yann Ferrand,[a] Cyril Poriel,[a] Paul Le Maux,[a] Joëlle Rault-Berthelot[b,*] and Gérard Simonneaux[a,*]

[a]*Laboratoire de Chimie Organométallique et Biologique, UMR CNRS 6509, Institut de Chimie, Université de Rennes 1, 35042 Rennes cedex, France*
[b]*Laboratoire d'Electrochimie Moléculaire et Macromoléculaire, UMR CNRS 6510, Institut de Chimie, Université de Rennes 1, 35042 Rennes cedex, France*

Received 7 January 2005; accepted 31 January 2005
Available online 11 March 2005

Abstract—Anodic oxidation of chiral ruthenium complexes of spirobifluorenylporphyrins leads to the coating of the working electrode by insoluble optically active films whose electrochemical behaviour and physicochemical properties are described. After removal from the electrode, the ruthenium-complexed polymers were evaluated as enantioselective catalysts for the cyclopropanation of olefins by ethyl diazoacetate. The results show the reactions proceeded very efficiently at room temperature with excellent yields (80–90%) and moderate enantioselectivities (up to 53% at −40 °C). The chiral electrosynthesized polymer catalysts can be recycled by simple filtration and reused even up to the seventh cycle with only a slight decrease of activity and enantioselectivity.

1. Introduction

The synthesis of enantiomerically pure compounds is one of the major challenges in heterogeneous catalysis.[1–4] The use of heterogeneous catalysts under ambient conditions offers several advantages compared with their homogeneous counterparts, such as ease of recovery and recycling and enhanced stability. Distinct methodologies have been developed for the immobilization of homogeneous catalysts or the creation of heterogeneous catalysts.[1] Thus, some of the commonly used metal-catalysts for asymmetric carbene transfer reactions have been immobilized on organic or inorganic supports, with a particular focus on bis(oxazoline)[5] and pyridine-bis(oxazoline) (pybox)[6,7] ligands. There are some recent reviews on this topic.[1,2,8,9] However most of the strategies have relied on covalent attachments between chiral ligands and the solid supports. A new strategy for the immobilization of rhodium catalysts has also been recently reported for cyclopropanation reaction.[10] Numerous methods for immobilizing metalloporphyrins under insoluble materials have been reported[11] but very few under optically active forms[12–15] and even less with success for asymmetric catalytic reactions.[14,15] We have recently shown that poly(tetraspirobifluorenylporphyrin) complexed by ruthenium showed potential applications as heterogeneous cyclopropanation catalysts of olefins with ethyl diazoacetate.[16] These polymers can be prepared by oxidative electropolymerization of metalloporphyrin complexes bearing spirobifluorene groups. Thus polymerization of Ru spirobifluoreneporphyrins leads to very efficient catalysts that can be easily recovered and reused. We anticipate that these heterogeneous catalytic systems would potentially be applicable to practical organic synthesis with a special focus on asymmetric catalysis using chiral polymers. As an extension of our previous work on polymers,[16] the spirobifluorenyl group was designed to allow polymerization and the chiral group for asymmetric induction. We chose a C_2-symmetric group, which contains two norbornane groups fused to the central benzene ring, previously reported by Halterman and Jan (Scheme 1).[17] This chiral group is particularly interesting since the enantiomeric excesses are quite high (90%) when the catalytic reactions are undertaken under homogeneous conditions.[18,19] Herein, we report the preparation of

* Corresponding authors. Tel.: +33 02 99286285; fax: +33 02 99281646; e-mail: gerard.simonneaux@univ-rennes1.fr

0957-4166/$ - see front matter © 2005 Published by Elsevier Ltd.
doi:10.1016/j.tetasy.2005.01.051

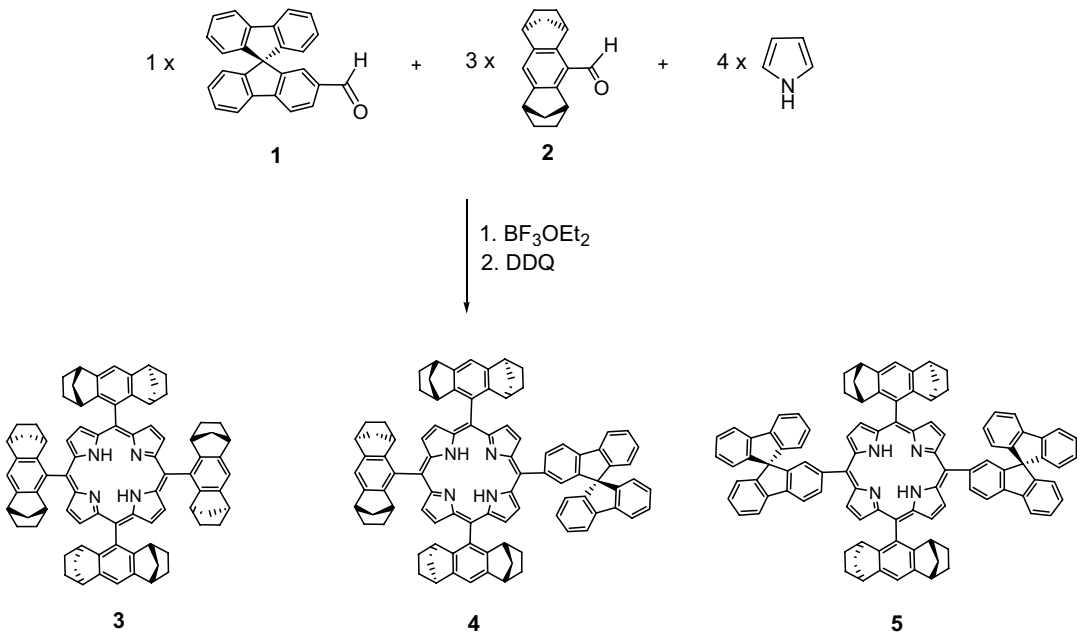

Scheme 1. Mixed aldehyde condensation of chiral dinorbornabenzaldehyde and 9,9′-spirobifluorene-2-carbaldehyde.

optically active electropolymers bearing chiral metalloporphyrins and asymmetric heterogeneous carbene transfer catalyzed by these polymers. To the best of our knowledge, this system is the first example, which shows asymmetric cyclopropanation with chiral polymers obtained by anodic oxidation as catalysts.

2. Results

2.1. Porphyrin and metalloporphyrin syntheses

We have previously reported the synthesis of the ruthenium complex of tetraspirobifluorenylporphyrin **TSP-RuCO**.[16] Due to possible difficulties (vide infra) with the polymerization of porphyrins bearing only one 9,9′-spirobifluorene group, we decided first to target porphyrins bearing two spirobifluorene groups. *trans*-A_2B_2 porphyrins are typically synthesized from 5-substituted dipyrromethane derivatives and aldehydes following the MacDonald [2+2] condensation.[20,21] Condensation of the 5-spirobifluorenyl-dipyrromethane with the chiral dinorbornabenzaldehyde in dichloromethane, in presence of a catalytic amount of BF_3OEt_2[22] gave a mixture consisting of at least four different tetraarylporphyrins, as shown by TLC. The major compounds were isolated in low yield (overall yields <10%) and identified by ^{1}H NMR spectroscopy and HRMS to be chiral porphyrins bearing 1–4 chiral groups.[19] It is almost certain that the mixture of porphyrins was produced as a result of acid redistribution reactions common of many dipyrromethanes, as previously reported by Smith and co-workers.[23]

An alternate route to these chiral porphyrins is also possible through a mixed-aldehyde condensation of spirobifluorene aldehyde, chiral aldehyde and pyrrole.[24] This method, which should afford a mixture of all the desired products was undertaken using a mixture of the two aldehydes, 9,9′-spirobifluorene-2-carbaldehyde **1** and dinorbornabenzaldehyde **2** in the ratio of 1/3 and pyrrole. This method gave a mixture of three porphyrins **3**, **4** and **5** in moderate yields (see Experimental). These porphyrins were readily separated to produce the two expected optically active porphyrins, **4** and **5** bearing three and two chiral groups, respectively (Scheme 1). The ruthenium complexes were then prepared by treatment of the porphyrins with Ru_3CO_{12} in degassed *o*-dichlorobenzene at 180 °C for 2 h to give **3-RuCO**, **4-RuCO** and **5-RuCO**. **3-RuCO** has previously been reported in 1997 by Berkessel and Frauenkron[25] and Che and co-workers.[26]

2.2. Electropolymerization and film formation

As recently reported with the tetraspirobifluorenylporphyrin ruthenium complex **TSP-RuCO**,[16] anodic oxidation of **4-RuCO** and **5-RuCO** yields the two reversible one-electron Ru-porphyrin oxidation ($E^1 \sim 0.4$ V and $E^2 \sim 0.8$ V vs Fc/Fc^+), corresponding to porphyrin and metal oxidation, respectively (see Table 1 and Fig. 1).[27,28] The ΔE between E^1 and E^2 is

Table 1. Three oxidation potentials of monomers **5-RuCO**, **4-RuCO** and **TSP-RuCO**

	E^{1a}	E^2	E^3
5-RuCO	0.44	0.86	1.34
4-RuCO	0.37	0.84	Shoulder[b]
TSPRuCO	0.46	0.89	1.37

All potentials were obtained during cyclic voltammetric investigations of **5-RuCO** (1.92×10^{-3} M), **4-RuCO** (4.58×10^{-3} M) and **TSP-RuCO** (2.2×10^{-3} M) in CH_2Cl_2 containing 0.2 M Bu_4NPF_6. Platinum electrode diameter 1 mm, sweep-rate: 100 mV/s.

[a] Potentials are referred to the ferrocene/ferrocenium.

[b] E^3 is a shoulder of a wave whose maximum is at 1.51 V.

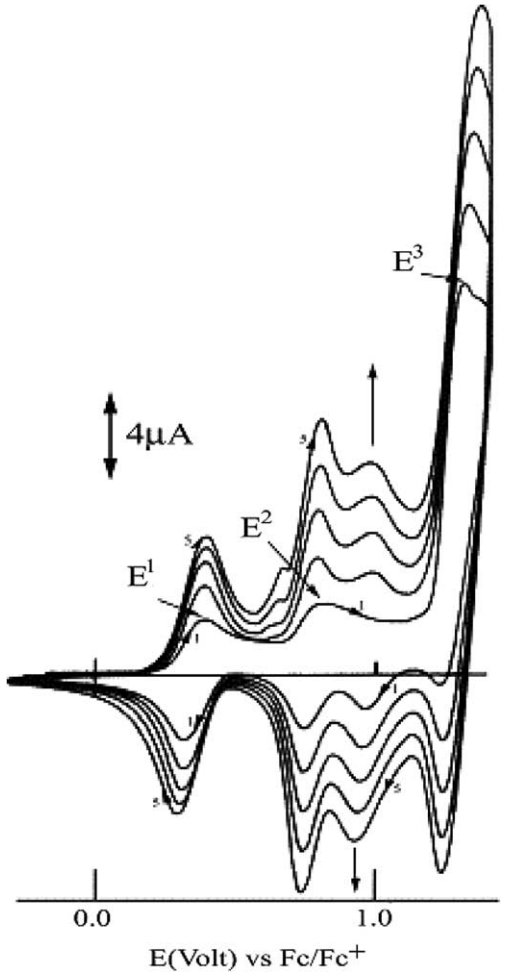

Figure 1. Cyclic voltammograms (CVs) recorded during the anodic oxidation of a 1.92×10^{-3} M solution of **5-RuCO** in CH_2Cl_2 and 0.2 M Bu_4NPF_6 using a Pt working electrode. Five sweeps between −0.32 and 1.5 V versus Fc/Fc^+. Sweep-rate: 100 mV/s.

~0.45 V for the three compounds. Then, irreversible spirobifluorene oxidation occurs at E^3 (~1.4 V). The intensity of this E^3 wave decreases from **TSP-RuCO > 5-RuCO > 4-RuCO** according to a decrease of the number of spirobifluorene units in the three compounds. Potentials of these redox couples are summarized in Table 1. No polymer film was observed on successive cycling if the potential sweep did not reach the third oxidation wave. In contrast, recurrent sweeps between −0.3 and 1.5 V versus Fc/Fc^+ led to a gradual modification of the cyclic voltammograms (CVs). After five recurrent sweeps, the CVs show the appearance of a new reversible wave around 1.0 V and the regular increase of the three waves E^1, E^2 and E^3.

The polymerization of **4-RuCO** (Fig. 6), bearing only one spirobifluorene unit, also leads to the appearance of the new reversible wave around 1.0 V versus Fc/Fc^+ but with a decrease in the intensity of the E^1 wave, which shifts towards a more positive potential. This is due to an increase of the threshold oxidation potential of this polymer, which is less easily p-doped because of the small amount of spirobifluorene units. After cycling, the electrode is covered by an insoluble 'gold like' film (Scheme 2), which can be studied in an electrolytic cell free of any electroactive species or can be scratched from the electrode to be used in heterogeneous catalytic reactions. Anodic copolymerizations of **4-RuCO** and **5-RuCO** were also performed in presence of 9,9′-spirobifluorene **SBF** using **SBF/4-RuCO** ratio of 1/4.2, 1/2.1 or 1/1.4, and **SBF/5-RuCO** of 1/4.8 or 1/2.3, respectively. The electrochemical behaviour, physicochemical properties and catalytic efficiencies of these copolymers were studied by comparison to poly(**4-RuCO**) and poly(**5-RuCO**).

2.3. Characterization of the polymer film

As shown in Figure 2, the CVs recorded in CH_2Cl_2 and Bu_4NPF_6 0.2 M with a platinum working electrode covered by poly(**5-RuCO**) gave two first oxidation waves in a potential range fitting the two one-electron oxidation waves of the Ru-porphyrin followed by two additional waves, which correspond to the p-doping process of the polyspirobifluorene units. The threshold oxidation potential of poly(**5-RuCO**) is 0.1 V versus Fc/Fc^+. In contrast, CVs recorded with a platinum electrode covered by poly(**4-RuCO**) (Fig. 3) show a threshold oxidation potential of poly(**4-RuCO**) at 0.58 V versus Fc/Fc^+. Therefore, the oxidation of the Ru-porphyrin unit occurs at a higher potential than in monomer **4-RuCO**, which is related to the beginning of the p-doping process of the polyspirobifluorene units. Thus, only one wave, including both oxidation processes, is observed in the CVs.

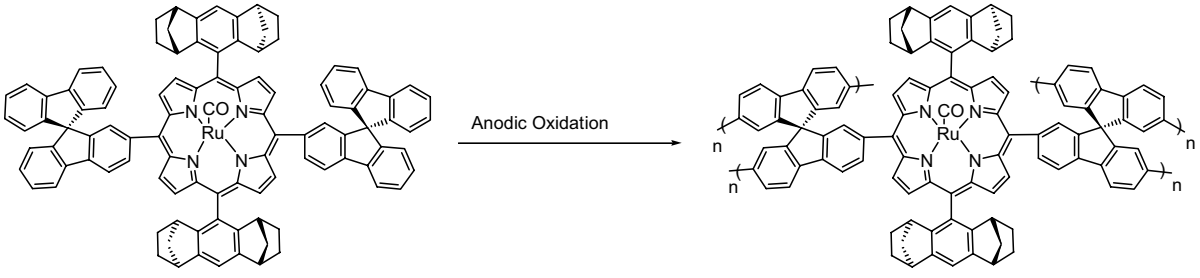

5-RuCO poly(**5-RuCO**)

Scheme 2. Anodic polymerization of **5-RuCO**.

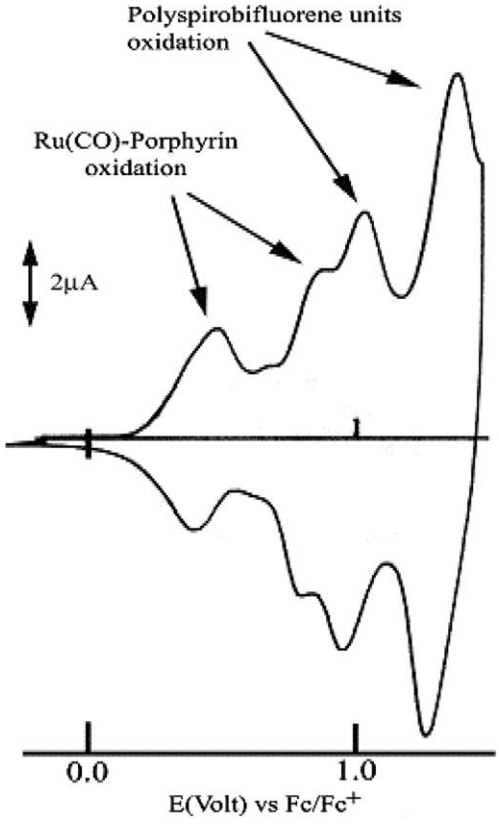

Figure 2. Cyclic voltammograms (CVs) recorded between −0.30 and 1.5 V in CH_2Cl_2 and 0.2 M Bu_4NPF_6 using a Pt working electrode modified by poly(**5-RuCO**), previously deposited by anodic oxidation at 1.44 V of a 1.92×10^{-3} M solution of **5-RuCO** in CH_2Cl_2 and 0.2 M Bu_4NPF_6, amount of charge used for the oxidation: 2×10^{-4} C. Sweep-rate: 100 mV/s.

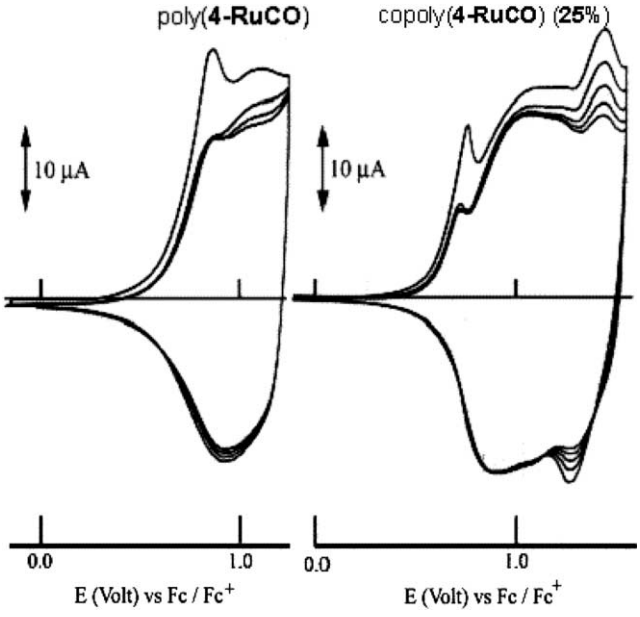

Figure 3. Cyclic voltammograms (CVs) recorded between −0.30 and 1.5 V in CH_2Cl_2 and 0.2 M Bu_4NPF_6 using a Pt working electrode modified by poly(**4-RuCO**) or copoly(**4-RuCO**) (25%), previously deposited by anodic oxidation at 1.44 V of a 1.92×10^{-3} M solution of **4-RuCO** in CH_2Cl_2 and 0.2 M Bu_4NPF_6, amount of charge used for the oxidation: 2×10^{-4} C. Sweep-rate: 100 mV/s.

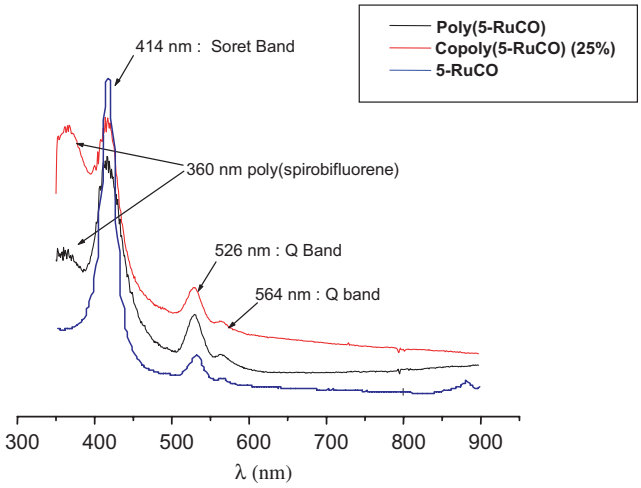

Figure 4. UV–vis spectra of **5-RuCO**, poly(**5-RuCO**) and copoly(**5-RuCO**) (25%) recorded in CH_2Cl_2. The insoluble deposits were previously coated on a platinum disc, which acts also as reflector for the optical beam.

Copoly(**4-RuCO**) (25%), obtained by copolymerization of **4-RuCO** with **SBF** (see Experimental), shows a threshold oxidation potential, which is shifted to a less positive potential: 0.48 V versus Fc/Fc^+ (Fig. 3). This is due to the higher amount of spirobifluorene units in the material and probably to the higher polyspirobifluorene chain length. The CVs present three oxidation waves. The first one, relatively sharp, was assigned to the first oxidation wave of the Ru-porphyrin. The second one, which appears larger, may include the second oxidation of the porphyrin and the first oxidation of the polyspirobifluorene p-doping process. Finally, the third sharper wave corresponds to the second wave of the p-doping process of the polyspirobifluorene units.

UV–vis absorption spectra of poly(**5-RuCO**) and copoly(**5-RuCO**) (**25**%) were performed for the comparison with the monomer **5-RuCO** (Fig. 4). The electronic spectrum of the polymers showed that the bands of the Ru-porphyrin at 414, 526 and 564 nm are maintained in the polymers together with an additional absorption band at 360 nm corresponding to the poly(spirobifluorene) units. The intensity of this band is higher in copoly(**5-RuCO**) (25%) than that in poly(**5-RuCO**) due to a higher content of spirobifluorene groups in the former.

2.4. Catalytic cyclopropanation reactions

We first choose to investigate the catalytic properties of the chiral ruthenium porphyrin monomers using the cyclopropanation of styrene (Table 2). Reactions were monitored by gas chromatography with asymmetric inductions determined by chiral gas chromatography. To assign the signals to the corresponding cyclopropane, we carried out the previously described homogeneous reaction,[29] allowing us to determine the enantiomeric excess in both *trans* and *cis* cyclopropanes, and also the absolute configuration of the products. With these reactive substrates, cyclopropanation yields

Table 2. Cyclopropanation of styrene with ethyl diazoacetate catalyzed by ruthenium catalysts[a]

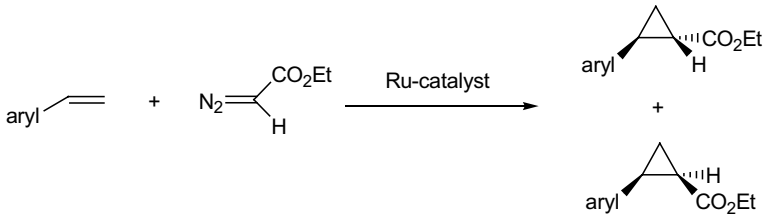

	Catalyst	Temperature (°C)	Yield (%)[b]	*trans*/*cis*	Ee_{trans}[c] (%) (1*S*,2*S*)	Ee_{cis}[c] (%) (1*S*,2*R*)
1	**3-RuCO**	25	96	95/5	87	4
2		−20	95	96/4	91	3
3	**4-RuCO**	25	95	93/7	65	3
4		−20	90	97/3	76	1
5	**5-RuCO**	25	94	90/10	41	8
6		−20	81	95/5	47	16

[a] Reactions were performed in CH_2Cl_2 for 24 h with a catalyst:diazo:substrate molar ratio of 1:200:1000.
[b] Yields were based on the styrene consumed.
[c] Determined by gas chromatography.

Table 3. Asymmetric cyclopropanation of styrene and ethyl diazoacetate catalyzed by porphyrins polymers[a]

	Catalyst	Solvent	Temperature (°C)	Yield[b] (%)	*trans*/*cis*	Ee_{trans}[c] (%) (1*S*,2*S*)	Ee_{cis}[c] (%) (1*S*,2*R*)
1	Copoly(**4-RuCO**) (25%)	Toluene	25	82	82/18	25	7
2			0	50	85/15	40	9
3			−40	35	77/23	53	7
4	Copoly(**5-RuCO**) (25%)		25	89	88/12	29	5
5			0	80	89/11	30	8
6	Copoly(**4-RuCO**) (25%)	CH_2Cl_2	25	86	87/13	22	5
7			0	79	81/19	28	5
8			−40	31	89/11	46	4
9	Copoly(**5-RuCO**) (25%)		25	89	89/11	29	9
10			0	85	90/10	29	6
11	Copoly(**4-RuCO**) (50%)		25	85	86/14	23	4
12			0	80	82/18	28	5

[a] Reactions were performed in CH_2Cl_2 for 24 h with a catalyst:diazo:substrate molar ratio of 1:200:1000.
[b] Yields were based on the styrene consumed.
[c] Determined by gas chromatography.

were higher than 90% with the two catalysts using ethyl diazoacetate. Obviously, monomer **3-RuCO** gave the highest enantioselectivity, due to the presence of four chiral groups (ee = 87%).[26] This enantioselectivity was increased at lower temperature (ee = 91%, −20 °C). Interestingly, complex **4-RuCO**, bearing only three chiral groups catalyzed the cyclopropanation with a moderate decrease of the ee (76%, −20 °C) by comparison with complex **3-RuCO**. A larger decrease was observed with complex **5-RuCO**, which bears only two chiral groups.

The solid polymers resulting from the electrocopolymerization of **4-RuCO** and 5-RuCO with SBF, copoly(**4-RuCO**) and copoly(**5-RuCO**), respectively, were then tested as catalysts in the cyclopropanation reactions of styrene with ethyl diazoacetate at three different temperatures (Table 3). Tables 2 and 3 allow the comparison of the results obtained with the homogeneous and the two different polymeric catalysts. The two polymers led to diastereoselectivities and yields (Table 3) close to those obtained with the homogeneous catalysts (Table 2). The solid obtained by the copolymerization of **4-RuCO** with spirobifluorene gave the best results in toluene, but the most significant difference with the monomer is the reduction of the enantioselectivity, decreasing from 76% (−20 °C) to 53% (−40 °C). If we expect this result at a low temperature, surprisingly, the two polymers gave similar enantioselectivity and diastereoselectivity. To illustrate the role that the polymeric matrix can play in the stereochemical outcome of reactions, copolymerization of **4-RuCO** with two different amounts of spirobifluorene was undertaken at two different temperatures (Table 3, entries 6, 7; 11, 12). Similar catalytic results were observed, showing that the dilution of the active site in the polymer seems not to modify the reactivity and the enantioselectivity.

The recovery and recyclability of copoly(**5-RuCO**) (25%) polymer were also examined. The polymer tested for enantioselectivity and reactivity in the cyclopropanation of styrene with ethyl diazoacetate could be used for seven recycling steps without a significant decrease in enantioselectivity or reactivity (Fig. 5). The yield decreased thought from 89% to 78% after seven runs while the enantioselectivity was maintained at ~30%.

3. Discussion

Asymmetric electrocatalytic reactions have recently been the subject of intense studies.[30,31] Thus, electrochemical asymmetric induction can be achieved by the use of chiral electrodes.[32–34] Various chiral polymers, mainly polythiophene[35] and polypyrrole derivatives,[30,36] have been described for the preparation of chiral electrodes capable of enantioselective recognition or electrosyntheses.[37] Although catalytic asymmetric reactions with chiral electropolymers have given some satisfactory results,[38] in no case were the polymers removed from the electrode. We report herein the development of novel chiral electropolymers for asymmetric heterogeneous carbene transfer to olefins.

Optically active ruthenium porphyrin complexes have been the focus of intense studies by us[19,29,39] and others[26,40–42] as catalysts for asymmetric cyclopropanation. In contrast, immobilizing chiral metalloporphyrins under insoluble materials is still rare.[14,15] Herein, we report a new method, using electropolymerization, to produce insoluble optically active polymers bearing ruthenium porphyrins, which can be used as heterogeneous asymmetric catalysts after being removed from the electrode.

3.1. Electrosynthesis and characterization

The mechanism of ruthenium porphyrin film formation is described below:

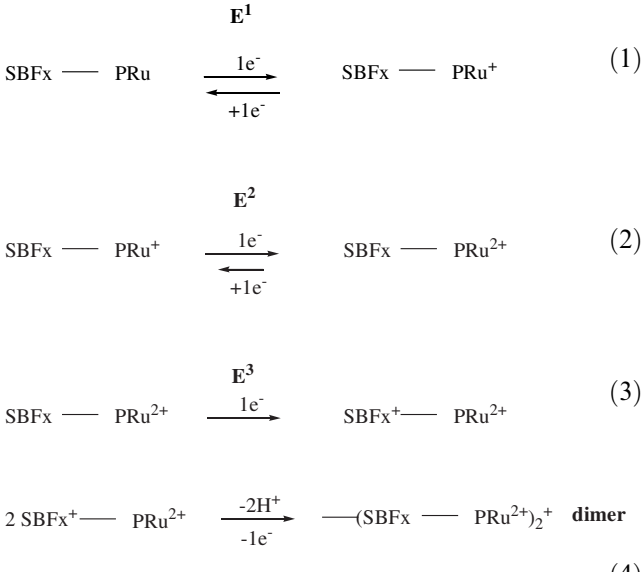

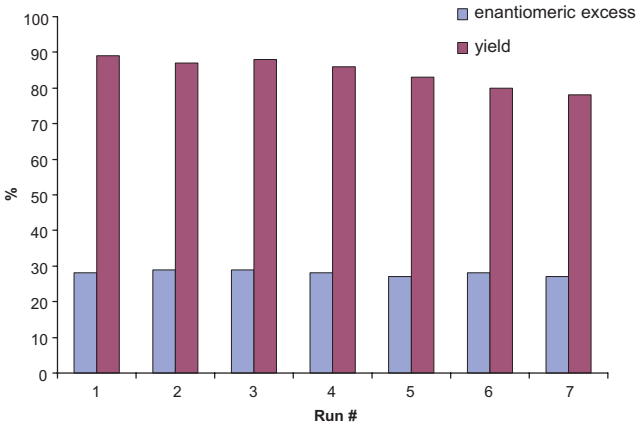

Figure 5. Recovery–reuse outcome from the cyclopropanation of styrene with ethyl diazoacetate using copoly(**5-RuCO**) (25%) as catalyst (CH_2Cl_2; 25 °C; catalyst loading: 5 mg).

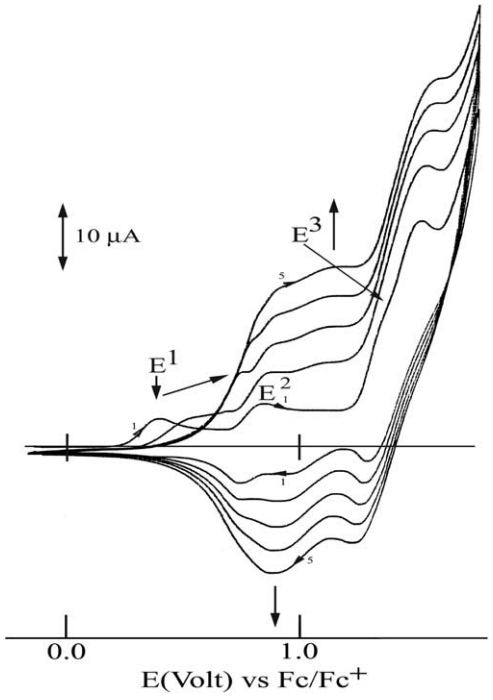

Figure 6. Cyclic voltammograms (CVs) recorded during the anodic oxidation of a 4.58×10^{-3} M solution of **4-RuCO** in CH_2Cl_2 + 0.2 M Bu_4NPF_6 using a Pt working electrode. Five sweeps between −0.2 and 1.7 V. Sweep-rate: 100 mV/s.

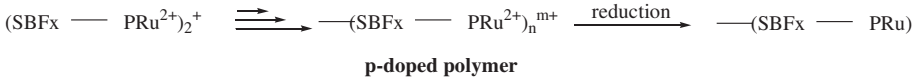

Metalloporphyrin film formation is suggested to be the two electron oxidation of the ruthenium porphyrin (Eqs. 1 and 2) followed by the oxidation of the spirobifluorene units to their radical cations (Eq. 3), which couple with other radicals via C2–C7 bonds. Next, two protons are eliminated at the C2 and C7 carbon atoms forming a dimer (Eq. 4). This dimer is immediately oxidized at this potential, since it is more easily oxidized

than the monomer, leading to a new dimer radical cation. Thus, the oligomer chain grows on the electrode surface, yielding a chiral ruthenium polyspirobifluorenylporphyrin with the ruthenium porphyrin in a high oxidation state. Before scratching the film out of the electrode, the oxidized polymer was electrochemically reduced at 0 V to give a neutral polymer.

It should be noted that the question of metal versus ring oxidation of ruthenium porphyrins for the second oxidation step (Eq. 2) is not obvious.[28,43] The doubly oxidized species is only stable on a cyclic voltammetry time scale, and it has been suggested that a rapid chemical reaction occurs after electrogeneration of this species.[28,43] Thus modified Pt disc electrodes, which were prepared by controlled-potential oxidation at 1.6 V, can be coated with a film containing ruthenium porphyrin with a partial lost of the carbon monoxide ligand. Accordingly, the IR spectrum of poly(**TSP-RuCO**) polymer showed a CO vibration at 1949 cm^{-1} in KBr very close to the value observed for the monomer, but with a relative reduced intensity (Fig. 7). The UV–vis spectrum suggests however that most of the porphyrin units in the polymers have a ruthenium atom in the +2 oxidation state since the Soret band is detected at 414 nm, as observed for the starting ruthenium monomer.

Copolymerization with free spirobifluorene was necessary to obtain larger amount of polymer with **4-RuCO**, the monomer containing only one spirobifluorene group. As expected, the polymerization ability of the different monomers increases with the number of spirobifluorene groups linked to the porphyrin ring. Moreover, the comparison of the values of the threshold oxidation of poly(**4-RuCO**) (0.58 V) and poly(**5-RuCO**) (0.1 V) suggests a possible conjugation through the metalloporphyrin units, which exists only in poly(**5-RuCO**). The less important negative shift of potential (0.1 V), observed from poly(**4-RuCO**) to copoly(**4-RuCO**) is due only to an increase of the polyspirobifluorene chain length.

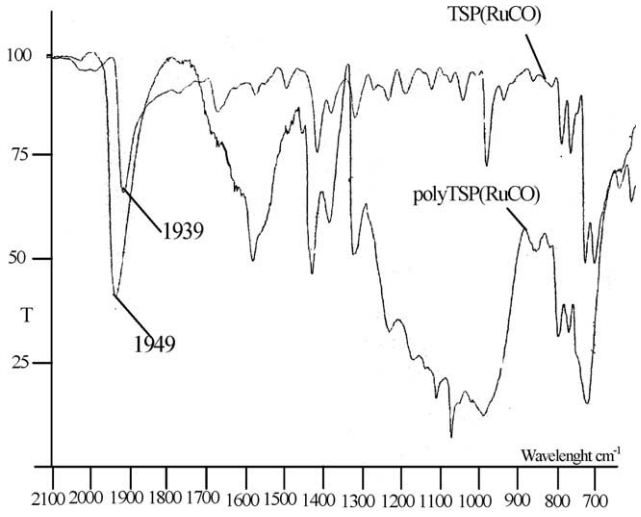

Figure 7. Infra-red spectra of the monomer **TSP-RuCO** and its polymer: poly(**TSP-RuCO**).

3.2. Heterogeneous catalysis

We reported in a preliminary communication[16] that ruthenium spirobifluorenylporphyrins can be electropolymerized and then used as carbene transfer catalysts. Herein, we have prepared new optically active polymers by electropolymerization of chiral ruthenium porphyrins. The good stability of these catalysts is obvious if we consider the recovery and the enantioselectivity after seven cycles, as reported in Figure 5. No significant metal porphyrin leaching was observed during these heterogeneous reactions. To prepare the catalytic system, it was necessary to introduce a nonchiral group, the spirobifluorene, to polymerize the monomer. Obviously, a decrease in the enantiomeric excess is to be expected if we compared the catalytic efficiency, **3-RuCO > 4-RuCO > 5-RuCO** under homogeneous conditions, according to the number of chiral groups. It was thought that complex **4-RuCO**, bearing only three chiral groups catalyzed the cyclopropanation with only a moderate decrease in the ee (76%, −20 °C) by comparison with complex **3-RuCO** (91%, −20 °C). In contrast, the enantioselectivity is reduced to 53% as the best result (Table 3, entry 3) after copolymerization of **4-RuCO**. It is difficult to give an explanation for this effect, although it is clear that the polymer has a different influence on the energy of the transition states of the reaction. This effect may also be related to a diminished access of the substrates to the catalytic sites because of the cross-linked structure of the polymers. It should be noted that atropisomers were detected with ruthenium spirobifluorenylporphyrins.[44] Another explanation would be the presence of high oxidation state ruthenium species in the polymer, such as paramagnetic Ru(III) and Ru(IV) as reactive species, in the case of incomplete reduction after the electropolymerization. This reactive sites may also decrease the enantioselectivity.

4. Conclusion

Despite the good stability and recyclability, the polymeric catalysts suffer from the drawback of moderate enantioselectivity compared to the homogeneous counterpart. Compared to another chiral ruthenium porphyrins immobilized in a sol–gel matrix used for asymmetric epoxidation in which catalyst leaching and deactivation were observed,[14] the system herein seems however to offer better recyclability. An alternative method to increase the enantioselectivity will be to attach the spirobifluorene groups at the periphery of the chiral porphyrin to maintain the local D_4 symmetry. Accordingly, recent promising results obtained with a D_4-chiral porphyrin encapsulated in ordered mesoporous molecular sieves,[15] have been reported for intramolecular cyclopropanation. We have developed a simple and efficient methodology for the immobilization of chiral porphyrin systems, which may also be used for the oxidation reaction. This new route opens the way for the preparation of a range of different supported chiral porphyrin-based catalysts for a wide variety of enantioselective reactions.

5. Experimental

5.1. General

All reactions were performed under argon and were magnetically stirred. Solvents were distilled from appropriate drying agent prior to use: Et_2O and THF from sodium and benzophenone, toluene from sodium, CH_2Cl_2 from CaH_2, $CHCl_3$ from P_2O_5 and all other solvents were HPLC grade. Commercially available reagents were used without further purification unless otherwise stated. All reactions were monitored by TLC with Merck pre-coated aluminium foil sheets (Silica gel 60 with fluorescent indicator UV_{254}). Compounds were visualized with UV light at 254 and 365 nm. Column chromatographies were carried out using silica gel from Merck (0.063–0.200 mm). ^1H NMR and ^{13}C NMR in $CDCl_3$ were recorded using Bruker (Advance 500dpx and 300dpx spectrometers) at 500 and 75 MHz, respectively. High-resolution mass spectra were recorded on a ZabSpec TOF Micromass spectrometer in ESI positif mode at the CRMPO.

All electrochemical experiments were performed using a platinum disc electrode [a Pt working electrode (diameter 1 mm) for CVs or a platinum sheet area (2 cm^2) for preparative electrosynthesis]. The counter electrode was a vitreous carbon rod and the reference electrode was a silver wire in a 0.1 M $AgNO_3$ solution in CH_3CN. Ferrocene was added to the electrolyte solution at the end of a series of experiments. The ferrocene/ferrocenium (Fc/Fc^+) couple served as internal standard and all reported potentials are referenced to its reversible formal potential. Activated Al_2O_3 was added in the electrolytic solution to remove excess moisture. The three electrodes cell was connected to a PAR Model 173 potentiostat monitored with a PAR Model 175 signal generator and a PAR Model 179 signal coulometer. The cyclic voltammetry traces (CVs) were recorded on an XY SEFRAM-type TGM 164.

Dichloromethane with less than 100 ppm of water (ref. SDS 02910E21) and tetrabutylammonium hexafluorophosphate from FLUKA were used without any purification. Aluminium oxide was obtained from Woëlm, activated by heating at 300 °C under vacuum for 12 h and used at once under argon pressure.

Liquid UV–vis spectra were recorded on a UVIKON XL from Biotech. Solid UV–vis spectra were recorded using a Guided Wave model 150 spectrophotometer with optical fibres; a concave platinum surface acted as a reflector for the optical beam. Infrared spectra were performed in KBr disc in a IFS 28 Bruker. All catalytic reactions were controlled on a Varian CP-3380 Gas Chromatograph equipped with a CP-Chirasil-Dex Column.

5.2. Synthesis of porphyrins

9,9′-Spirobifluorene-2-carbaldehyde (0.191 g, 0.556 mmol), dimethanoanthracene-9-carbaldehyde (0.4 g, 1.667 mmol) and pyrrole (155 μL, 2.2 mmol) were allowed to react at room temperature in dry and degassed chloroform (31 mL) under an argon atmosphere and protected from light, with acid catalysis (BF_3OEt_2: 70 μL, 0.49 mmol). Under these conditions, the reaction reached an equilibrium in about 2 h. A stoichiometric amount of DDQ was then added to irreversibly oxidize the porphyrinogene. After the addition of several drops of triethylamine and ordinary work-up, concentration, washing, drying, the crude reaction mixture was purified by chromatography on basic alumina (CH_2Cl_2/pentane: 1/1). The purple fraction, which eluted first, was a mixture of three different porphyrins based on TLC (pentane/CH_2Cl_2: 8/2): (R_f **3**: 0.82; R_f **4**: 0.56; R_f **5**: 0.30), which consisted, after chromatography on silica of porphyrins **3** (10%), **4** (18%) and **5** (8%).

5.3. 5,10,15,20-Tetrakis-[(1*S*,4*R*,5*R*,8*S*)-1,2,3,4,5,6,7,8-octahydro-1,4:5,8-dimethanoanthracene-9-yl]-porphyrin 3

The synthesis of this porphyrin was previously reported.[17]

5.4. 5,10,15-Tri-[(1*S*,4*R*,5*R*, 8*S*)-dimethanoanthracen-9-yl-]20-monospirobifluorenylporphyrin 4

^1H NMR ($CDCl_3$, ppm): −2.60 (s, 2H); 1.02 (m, 6H); 1.41 (m, 18H); 1.79 (m, 6H); 2.06 (m, 6H); 2.84 (m, 6H); 3.62 (s, 6H); 6.92 (d, 2H); 7.18 (td, 2H); 7.27 (m, 2H); 7.33 (t, 1H); 7.39 (t, 1H); 7.43 (m, 3H); 7.54 (t, 1H); 7.83 (m, 3H); 8.13 (d, 1H); 8.19 (dd, 2H); 8.76 (m, 8H). UV–vis (CH_2Cl_2): λ_{max}/nm ($\log\varepsilon$): 224 (4.78); 274 (4.54); 423 (5.38); 517 (4.17); 553 (3.87); 592 (3.79); 647 (3.61); Mass (ESI, CH_2Cl_2/MeOH 9/1) (*m*/*z*): calculated for $C_{93}H_{77}N_4$ $[M+H]^+$: 1249.6148; found: 1249.6129.

5.5. 5,15-Bis-[(1*S*,4*R*,5*R*,8*S*)-dimethanoanthracen-9-yl-]10,20-bis-spirobifluorenylporphyrin 5

^1H NMR ($CDCl_3$, ppm): −2.78 (s, 2H); 1.18 (m, 4H); 1.35 (m, 12H); 1.86 (m, 4H); 2.00 (m, 4H); 2.98–2.42 (m, 4H); 3.57 (s, 4H); 6.89 (t, 2H); 7.06 (m, 5H); 7.26 (m, 5H); 7.38 (m, 5H); 7.52 (t, 2H); 7.69 (d, 1H); 7.78 (m, 5H); 7.98 (d, 1H); 8.09 (m, 3H); 8.16 (m, 3H); 8.66 (m, 8H). UV–vis (CH_2Cl_2): λ_{max}/nm ($\log\varepsilon$) 227 (4.83); 270 (4.58); 308 (4.42); 423 (5.41); 517 (4.11); 553 (3.90); 591 (3.65); 647 (3.60). Mass (ESI, CH_2Cl_2/MeOH 9/1) (*m*/*z*): calculated for $C_{102}H_{75}N_4$ $[M+H]^+$: 1355.7142 found: 1355.7135. Since compound **5** and the major compound (containing two chiral groups) obtained from the MacDonald condensation showed the same NMR spectrum, it is assumed that the two chiral groups are in the *trans*-position.

5.6. 5,10,15-Tri-[(1*S*,4*R*,5*R*,8*S*)-dimethanoanthracen-9-yl-]20-monospirobifluorenyl porphyrinatorutheniumcarbonyl 4-RuCO

To a solution of **4** (100 mg, 0.08 mmol) dissolved in degassed *o*-dichlorobenzene heated at 180 °C, was added by portion, Ru_3CO_{12} (153 mg, 0.24 mmol). The mixture was stirred under an argon atmosphere for 2 h until the reaction was completed. The solvent was removed under

high vacuum and the crude product was purified by chromatography on silica gel using first pentane, then a mixture of pentane/dichloromethane (1/1). The major red-orange band was collected and dried under vacuum to afford a red powder. Yield 90%. ^{1}H NMR ($CDCl_3$, ppm): 1.30 (m, 24H); 1.87 (m, 6H); 1.99 (m, 6H); 2.71 (m, 6H); 3.58 (s, 6H); 6.87 (t ; 1H); 7.12 (m; 2H); 7.24 (m, 2H); 7.36 (m, 6H); 7.53 (m, 1H); 7.65 (d, 1H); 7.77 (dd, 2H); 8.20 (m, 3H); 8.54 (m, 8H). UV–vis (CH_2Cl_2): λ_{max}/nm ($\log\varepsilon$): 224 (4.88); 308 (4.47); 413 (5.38); 529 (4.35). Mass (ESI, CH_2Cl_2/MeOH 9/1) (*m*/*z*): calculated for $C_{94}H_{75}N_4O$ ^{102}Ru $[M+H]^+$: 1377.4984 found: 1377.5053; IR (KBr): ν_{CO} = 1943.9 cm^{-1}.

5.7. 5,15-Bis-[(1*S*,4*R*,5*R*,8*S*)-dimethanoanthracen-9-yl-]10,20-bis-spirobifluorenyl porphyrinatorutheniumcarbonyl 5-RuCO

The complex was prepared using the same method as for compound **4-RuCO**. Yield 90%. ^{1}H NMR ($CDCl_3$, ppm): 8.49 (m, 8H); 8.18 (m, 4H); 8.09 (m, 2H); 7.75 (m, 4H); 7.52 (m, 4H); 7.35 (m, 6H); 7.24 (m, 5H); 7.11 (m, 5H); 6.87 (m, 2H); 3.55 (br s, 4H); 2.74–2.52 (m, 4H); 1.91 (m, 8H); 1.34 (m, 12H); 1.11 (m, 4H). UV–vis (CH_2Cl_2): λ_{max}/nm ($\log\varepsilon$) 228 (5.15); 308 (4.81); 415 (5.35); 530 (4.34). Mass (ESI, CH_2Cl_2/MeOH 9/1) (*m*/*z*): calculated for $C_{103}H_{72}N_4ONa$ ^{102}Ru $[M+Na]^+$: 1505.4647 found: 1505.4610; IR (KBr): ν_{CO} = 1943.9 cm^{-1}.

Synthesis and spectroscopic data of tetrasubstituted spirobifluorenylporphyrin ruthenium carbon monoxide, **TSP-RuCO** were reported in a previous paper.[16]

5.8. Copolymerization

Anodic copolymerizations of **4-RuCO** and **5-RuCO** were performed in presence of 9,9′-spirobifluorene (**SBF**) using either **SBF/4-RuCO** ratio of 1/4.2, 1/2.1 (w/w) or **SBF/5-RuCO** of 1/4.8 or 1/2.3 (w/w), respectively.

For clarity, the following abbreviations were used to name the copolymer:

SBF/4-RuCO
Ratio 1/4.2:copoly(**5-RuCO**) (25%)
Ratio 1/2.1:copoly(**5-RuCO**) (50%)
SBF/5-RuCO
Ratio 1/4.8:copoly(**4-RuCO**) (25%)
Ratio 1/2.3:copoly(**4-RuCO**) (50%)

5.9. Catalytic conditions for monomers

The catalyst (0.5%) was placed in an oven-dried haemolysis tube. This tube was evacuated, and backfilled with argon. The solvent (1 mL) was added via syringe, followed by the alkene (1 mmol). Next the diazo (0.2 mmol) was added slowly to the mixture over a period of 30 min. After 2 h for ethyl diazoacetate, the resulting mixture was evaporated and purified by flash silica gel chromatography to give the product.

5.10. Catalytic conditions for polymers

Conditions are similar to those with monomers. Catalyst amounts used were calculated from the Ru contents in the heterogeneous catalysts and determined by electronic microanalysis. After 2 h, the mixture was filtered and the residue washed several times by acetone and dichloromethane. The polymer was dried under vacuum and used for another run under the same experimental conditions.

5.11. Enantiomeric excess determination

For the cyclopropyl esters obtained from cyclopropanation of styrene with ethyl diazoacetate: GC-column CP-Chirasil-Dex column, injector 200 °C (pulsed split mode), detector (FID 220 °C, oven: 120 °C; 2.5 °C min^{-1}), pressure = 15 psi. *cis* (1*R*,2*S*) τ_r = 13.30 min; *cis* (1*S*,2*t*) τ_r = 13.78 min; *trans* (1*R*,2*R*) τ_r = 14.21 min; *trans* (1*1S*,2*S*) τ_r = 14.36 min.

Acknowledgments

We thank Girex and the MENRT for financial support (Y.F. and C.P.).

References

1. Rechavi, D.; Lemaire, M. *Chem. Rev.* **2002**, *102*, 3467–3494.
2. Fan, Q. H.; Li, Y. M.; Chan, A. S. C. *Chem. Rev.* **2002**, *102*, 3385–3466.
3. Bräse, S.; Lauterwasser, F.; Ziegert, R. E. *Adv. Synth. Catal.* **2003**, *345*, 869–929.
4. McMorn, P.; Hutchings, G. J. *Chem. Soc. Rev.* **2004**, *33*, 108–122.
5. Burguete, M. I.; Fraile, J. M.; Garcia, J. I.; Garcia-Verdugo, E.; Luis, S. V.; Mayoral, J. A. *Org. Lett.* **2000**, *2*, 3905–3908.
6. Annunziata, R.; Benaglia, M.; Cinquini, M.; Cozzi, F.; Pitillo, M. *J. Org. Chem.* **2001**, *66*, 3160–3166.
7. Cornejo, A.; Fraile, J. M.; Garcia, J. I.; Garcia-Verdugo, E.; Gil, M. J.; Luis, S. V.; Martinez-Merino, V.; Mayoral, J. A. *Org. Lett.* **2002**, *4*, 3927–3930.
8. Davis, M. E. *Top. Catal.* **2003**, *25*, 3–7.
9. MacMorn, P.; Hutchings, G. J. *Chem. Soc. Rev.* **2004**, *33*, 108–122.
10. Davies, H. M. L.; Walji, A. M.; Nagashima, T. *J. Am. Chem. Soc.* **2004**, *126*, 4271–4280.
11. Poriel, C.; Ferrand, Y.; Le Maux, P.; Rault-Berthelot, J.; Simonneaux, G. *Inorg. Chem.* **2004**, *43*, 5086–5095.
12. Geier, G. R., III; Sazaki, T. *Tetrahedron* **1999**, *55*, 1859–1870.
13. Geier, G. R., III; Lybrand, T. P.; Sazaki, T. *Tetrahedron* **1999**, 1871–1880.
14. Zhang, R.; Yu, W. Y.; Wong, K. Y.; Che, C. M. *J. Org. Chem.* **2001**, 8145–8153.
15. Zhang, J. L.; Liu, Y. L.; Che, C. M. *Chem. Commun.* **2002**, 2906–2907.
16. Poriel, C.; Ferrand, Y.; Le Maux, P.; Paul, C.; Rault-Berthelot, J.; Simonneaux, G. *Chem. Commun.* **2003**, 2308–2309.
17. Halterman, R. L.; Jan, S. T. *J. Org. Chem.* **1991**, *56*, 5253–5254.

18. Che, C. M.; Huang, J. S.; Lee, F. W.; Li, Y.; Lai, T. S.; Kwong, H. L.; Teng, P. F.; Lee, W. S.; Lo, W. C.; Peng, S. M.; Zhou, Z. Y. *J. Am. Chem. Soc.* **2001**, *123*, 4119–4129.
19. Ferrand, Y.; Le Maux, P.; Simonneaux, G. *Org. Lett.* **2004**, *6*, 3211–3214.
20. Arsenault, G. P.; Bullock, E.; MacDonald, S. F. *J. Am. Chem. Soc.* **1960**, *82*, 4384.
21. Rao, P. D.; Dhanalekshmi, S.; Littler, B. J.; Lindsey, J. S. *J. Org. Chem.* **2000**, *65*, 7323–7344.
22. Halterman, R. L.; Mei, X. *Tetrahedron Lett.* **1996**, *37*, 6291–6294.
23. Wallace, D. M.; Leung, S. H.; Senge, O. M.; Smith, K. M. *J. Org. Chem.* **1993**, *58*, 7245–7257.
24. Lindsey, J. S.; Prathapan, S.; Johnson, T. E.; Wagner, R. W. *Tetrahedron* **1994**, *50*, 8941–8968.
25. Berkessel, A.; Frauenkron, M. *J. Chem. Soc., Perkin Trans.* **1997**, 2265–2266.
26. Lo, W. C.; Che, C. M.; Cheng, K. F.; Mak, T. C. W. *J. Chem. Soc., Chem. Commun.* **1997**, 1205–1206.
27. Rillema, D. P.; Nagle, J. K.; Barringer, L. F.; Meyer, T. J. *J. Am. Chem. Soc.* **1981**, *103*, 56–62.
28. Mu, X. H.; Kadish, K. M. *Langmuir* **1990**, *6*, 51–56.
29. Galardon, E.; Le Maux, P.; Simonneaux, G. *J. Chem. Soc., Chem. Commun.* **1997**, 927–928.
30. Schwientek, M.; Pleus, S.; Hamann, C. H. *J. Electroanal. Chem.* **1999**, *461*, 94–101.
31. Guo, P.; Wong, K. Y. *Electrochem. Commun.* **1999**, *1*, 559–563.
32. Tallec, A. *Bull. Soc. Chim. Fr.* **1985**, *5*, 743–761.
33. Papillon, J.; Schulz, E.; Gélinas, S.; Lessard, J.; Lemaire, M. *Synth. Met.* **1998**, *96*, 155–160.
34. Rault-Berthelot, J.; Raoult, E.; Tahri-Hassani, J.; Le Deit, H.; Simonet, J. *Electrochim. Acta* **1999**, *44*, 3409–3419.
35. Lemaire, M.; Delabouglise, D.; Garreau, R.; Guy, A.; Roncali, J. *J. Chem. Soc., Chem. Commun.* **1988**, 658–661.
36. Pleus, S.; Schwientek, M. *Synth. Met.* **1998**, *95*, 233–238.
37. Cosnier, S.; Le Pellec, A.; Marks, R. S.; Périé, K.; Lellouche, J. P. *Electrochem. Commun.* **2003**, *5*, 973–977.
38. Komori, T.; Nonaka, T. *J. Am. Chem. Soc.* **1984**, *106*, 2656–2659.
39. Simonneaux, G.; Le Maux, P. *Coord. Chem. Rev.* **2002**, *228*, 43–60.
40. Frauenkron, M.; Berkessel, A. *Tetrahedron Lett.* **1997**, *38*, 7175–7176.
41. Gross, Z.; Galili, N.; Simkhovich, L. *Tetrahedron Lett.* **1999**, *40*, 1571–1574.
42. Che, C. M.; Huang, J. S. *Coord. Chem. Rev.* **2002**, *231*, 151–164.
43. Brown, G. M.; Hopf, F. R.; Ferguson, J. A.; Meyer, T. J.; Whitten, D. G. *J. Am. Chem. Soc.* **1973**, *95*, 5939–5942.
44. Poriel, C.; Ferrand, Y.; Juillard, S.; Le Maux, P.; Simonneaux, G. *Tetrahedron* **2004**, *60*, 145–158.